PCCP

Cite this: *Phys. Chem. Chem. Phys.*, 2012, **14**, 964–971

www.rsc.org/pccp

PAPER

Water diffusion inside carbon nanotubes: mutual effects of surface and confinement

Yong-gang Zheng,[a] Hong-fei Ye,[a] Zhong-qiang Zhang[ab] and Hong-wu Zhang*[a]

Received 15th August 2011, Accepted 8th November 2011
DOI: 10.1039/c1cp22622c

The mutual effects of two crucial features of carbon nanotubes (CNTs) (surface and confinement) on the temperature-dependent water diffusion are studied through molecular dynamics simulations. A two-stage diffusion mechanism is detected in the CNTs of diameter smaller than 12.2 Å, which becomes obscure as the temperature increases. This peculiar phenomenon can be ascribed to the cooperation of the small confinement and the periodic surface. The diffusion coefficient of the confined water exhibits a nonmonotonic dependence on the confinement size and an unexpected increase inside the large CNTs (compared to that of bulk water). These anomalous behaviors can be attributed to the competition of the smooth surface and the small confinement. Considering the mutual effects, an empirical formula is proposed on the basis of two groups of numerical examples, whose results indicate that the confinement effect will dominate over the surface effect until the CNT diameter increases up to ~16 Å, whereas thereafter the surface effect becomes dominant and finally both of them vanish gradually.

1. Introduction

The dynamics behaviors of fluid molecules can be characterized by the fundamental transport property, such as diffusion and viscosity. Compared with the fluids in the bulk phase, the special surface (patterned and smooth) and the nanoscale confinement can induce a dramatic change in the transport property of fluids in nanochannels.[1–8] Moreover, inside the channels of size comparable to molecular diameter, the molecular thermal fluctuations play an unforeseen role for the equilibrium property of fluids.[9–13] These unpredictable factors lead to that the conventional understanding of the macroscopic fluids may be no longer applicable for the fluids confined in nanochannels,[14,15] which restricts the application and the development of the nanofluidics system. Hence, the fundamental transport property such as the diffusion behavior of fluids at the nanoscale requires further understanding and reevaluation.

Generally, the diffusion behavior can be examined through the scaling relationship between the mean square displacement (MSD) and the exponent of time.[1,2,16] The scale factor and the time exponent reflect the molecular mobility and the diffusion mechanism, respectively. For bulk fluids, molecular motions follow the Fickian diffusion mechanism, in which the MSD linearly scales with time.[17] Besides this ubiquitous diffusion mechanism, two anomalous diffusion mechanisms can also be observed in some ideal and limiting cases. An ideal system, in which the molecules can move with an approximately constant velocity, will experience a ballistic diffusion (the MSD scales with the square of time).[18] Conversely, a compact system, in which the molecules densely assemble in a chain-like structure and cannot pass each other, will experience a single-file diffusion (the MSD scales with the square root of time),[19] which has been widely verified by the experimental and theoretical studies of one-dimensional flow in nanochannels.[20–33]

Carbon nanotube (CNT) is a promising candidate as a nanochannel due to its perfect structure and excellent mechanical properties. Recently, the fluid diffusions inside CNTs have attracted much attention. For one-dimensional water chain, the single-file diffusion mechanism has been observed inside the (6, 6) nanoring and the infinitely long (6, 6) CNT in long-time diffusion.[8,28] However, the (6, 6) CNT of finite length only supports the Fickian-type diffusion, which can be ascribed to the finite residence time of water molecules inside the CNT.[29] The molecular dynamics (MD) simulations of water confined in the (8, 8) CNT revealed an initial ballistic diffusion lasting for 500 ps, and thereafter the Fickian diffusion prevails.[2] It was pointed out that the long-lasting hydrogen bonds are responsible for the long-time ballistic diffusion. For the oxygenated (8, 8) carbon nanotubes, water diffusion undergoes a transition from little diffusion to Fickian diffusion as the water density increases from about 0.022 to 0.412 g cm^{-3}.[16] As for the large CNTs, the diffusion coefficient describing the molecular mobility under

[a] *State Key Laboratory of Structural Analysis for Industrial Equipment, Department of Engineering Mechanics, Faculty of Vehicle Engineering and Mechanics, Dalian University of Technology, Dalian 116023, China. E-mail: zhanghw@dlut.edu.cn; Fax: +86-411-84706249; Tel: +86-411-84706249*
[b] *Center of Micro/Nano Science and Technology, Jiangsu University, Zhenjiang 212013, China*

the Fickian diffusion mechanism can be calculated through the linear MSD–t relation. Nanok *et al.* computed the diffusion coefficient of water confined in CNTs of diameter varying from 12 to 27 Å.[30] The computational results indicated that the diffusion coefficient of the confined water increases with increasing diameter of CNTs and gradually approaches that of bulk water, whose trend is almost consistent with the results inside the similar CNTs with a constant water density.[4,10] The calculation of the diffusion coefficient based on the CNTs of diameter 7–21 Å revealed an obvious decrease in the diffusion coefficient inside the CNTs of diameter about 10 Å.[34] In our previous work we studied the water diffusion inside the CNTs of diameter in a wide range of 8–54 Å under a natural hydrostatic pressure at room temperature, where emphasis was placed on the size dependence of the diffusion mechanism and the diffusion coefficient of the confined water.[8] Moreover, Liu *et al.* proposed an estimation formula with two undetermined coefficients for the temperature-dependent diffusion coefficient of fluids inside the nanopores, which was applied to the polar water molecules inside the pores of width 12–25 Å.[12]

As mentioned above, most of the previous works were focused on the diffusion behavior within a small diameter range (9–27 Å), which cannot yet shed light on the size dependence of the diffusion mechanism and the diffusion coefficient. Furthermore, the temperature effect on the diffusion behavior of the water inside the CNTs was seldom studied. Especially, it should be noted that the special surface (patterned and smooth) and the small confinement are two important features of CNTs, which play crucial roles in the diffusion behaviors. The research on the mutual effects of the two crucial factors on the diffusion behaviors should be significant for recognizing the transport property and the flow behavior at the nanoscale.

In this paper, the diffusion mechanism and the diffusion coefficient of the water molecules inside CNTs of diameter ranging from 8 to 54 Å are studied by the MD simulations. The computations are conducted at different temperatures (298 K, 325 K and 350 K) to explore temperature dependence of diffusion behavior. Here, the extraordinary diffusion behavior of water molecules is explained by the mutual effects of the special surface and the small confinement of CNTs, which are verified by two groups of numerical examples, respectively. The surface effect is probed by changing the interactions between the water molecules and the nanotube atoms, while the confinement effect is identified by considering three kinds of CNTs with similar ratios of surface to volume but different cross-sections (diamond, square and circle).

2. Computational model

In this work, the simulation system is constructed by an armchair single-walled CNT and the water molecules of a specified amount, as shown in Fig. 1. The diameter of CNTs ranges from 8 Å to 54 Å, correspondingly, the length of CNTs varies from 2361 Å to 79 Å. The detailed sizes of the computational models are listed in Table 1. For the small CNTs, the ultra-long length is to ensure that enough water molecules can be contained so as to obtain enough statistical samples. To reduce the computational consumption, the CNTs are considered as rigid channels through fixing the carbon atoms. The water molecules are simulated by the TIP4P-EW model,[35] as shown in Fig. 1. The bond length and the angle of water molecules are 0.9572 Å and 104.52°, respectively, which are constrained by the SHAKE algorithm during the simulation process. The densities of water inside the CNTs at the three temperatures are presented in Fig. 2,[13] which are determined through a preparative MD model composed of a CNT and two water reservoirs. The MD simulations are carried out by an open-source code LAMMPS.[36]

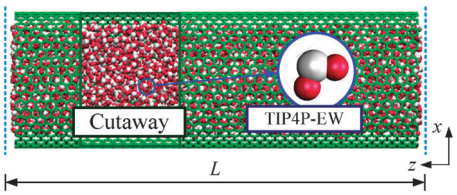

Fig. 1 The illustration of the computational model of the (24, 24) CNT. An interior snapshot and the TIP4P-EW water model are given. The dashed lines on both sides of the CNT represent the periodic boundary. The length of the CNT in a periodicity is *L*.

Table 1 The detailed sizes of the computational models

Chirality	Diameter/Å	The length of CNTs/Å
(6, 6)	8.14	2361.13
(7, 7)	9.50	1234.06
(8, 8)	10.84	683.74
(9, 9)	12.20	506.66
(10, 10)	13.56	371.39
(11, 11)	14.92	292.68
(12, 12)	16.28	226.28
(16, 16)	21.70	110.68
(20, 20)	27.12	103.30
(24, 24)	32.54	98.38
(30, 30)	40.68	88.54
(40, 40)	54.24	78.70

To examine the temperature effect on the diffusion behavior of the water confined in CNTs, the present MD simulations are conducted at 298 K, 325 K and 350 K, respectively. The canonical ensemble (NVT) is adopted to update the positions and the velocities of the atoms with the integration time step of 1 fs. The constant temperature is controlled by a Nose/Hoover thermostat. The interactions between the carbon atoms and the oxygen atoms of water molecules are calculated by the Lennard-Jones (LJ) potential with the parameters σ_{CO} = 3.28218 Å and ε_{CO} = 0.11831 kcal mol^{-1}.[8] The cutoff

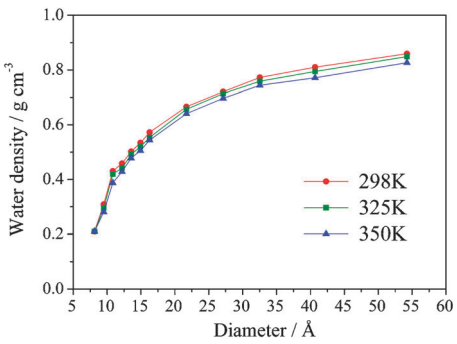

Fig. 2 The density of water inside the CNTs at 298 K, 325 K and 350 K.[13]

distances for the LJ interactions and the Coulomb energy are 10 Å and 12 Å, respectively. The particle–particle particle–mesh method is employed to compute the long-range Coulombic interactions. In the flow (axial) direction, the periodic boundary condition is applied to mimic an infinitely long CNT, which can overcome the boundary effect of CNT and obtain a long residence time for water molecules inside the CNTs. In the non-flow direction, due to the long-range Coulombic interactions, the periodic boundary condition is still required. Here, to reduce the interactions from the periodic cells in the non-flow directions, a huge vacuum is utilized to wrap around the CNT. The simulation time for the small-diameter CNTs (diameter <12.20 Å) is 10 ns and the data are collected in the last 8.5 ns. The computational results are averaged by six independent simulations with different initial configurations and velocities. While for the larger CNTs, the MD simulations are run for 5.5 ns and the data are collected in the last 5 ns. These simulations are repeated three times to eliminate the effect of initial conditions.

3. Diffusion mechanism

The diffusion mechanism of fluid molecules can be reflected by the scaling relationship between the MSD and the time,

$$\langle |\vec{r}(t) - \vec{r}(0)|^2 \rangle \propto At^{\alpha} \qquad (1)$$

where $\langle |\vec{r}(t) - \vec{r}(0)|^2 \rangle$ is the MSD which can be extracted from the MD simulations, $\langle\rangle$ denotes an average over all the molecules, $|\vec{r}(t) - \vec{r}(0)|$ is the displacement of a molecule during the time interval t. In the present equilibrium MD simulations, the drift of the mass center of all the water molecules is subtracted in the MSD calculation. A is the scale factor describing molecular mobility and α is the time exponent indicating the diffusion mechanism of fluid molecules. $\alpha = 1$ represents the Fickian diffusion, which is the intrinsic diffusion mechanism of the bulk fluids. $\alpha = 0.5$ and $\alpha = 2$ correspond to the single-file and the ballistic diffusion mechanisms, respectively. The intermediate states $\alpha > 1$ and $\alpha < 1$ are referred to as the superdiffusion and the subdiffusion, which mean the molecular motions are faster and slower than the linearly time-dependent diffusion behavior, respectively.[37]

Fig. 3 depicts the logarithmic plot of the axial MSD of the water molecules inside the small-diameter ((6, 6), (7, 7), (8, 8) and (9, 9)) CNTs *versus* the time at 298 K,[8] 325 K and 350 K. The representative lines of the three preceding diffusion mechanisms are also given in Fig. 3. From the figure, it can be seen that all the curves reveal an initial ballistic diffusion up to a few tens of femtoseconds, which is a normal phenomenon for the diffusion behavior.[2] Subsequently, the water molecules inside the small-diameter CNTs follow a two-stage diffusion mechanism. In the first stage (short-time diffusion), the water molecules inside the (6, 6) and (7, 7) CNTs obey a slight superdiffusion at 298 K and 325 K. As the temperature increases to 350 K, the diffusion inside the (6, 6) CNT gradually approaches the Fickian diffusion mechanism while inside the (7, 7) CNT it still follows the superdiffusion mechanism. The motions of the water molecules inside the (8, 8) and (9, 9) CNTs in short time undergo a transition from the subdiffusion to the Fickian diffusion mechanism with increasing temperature.

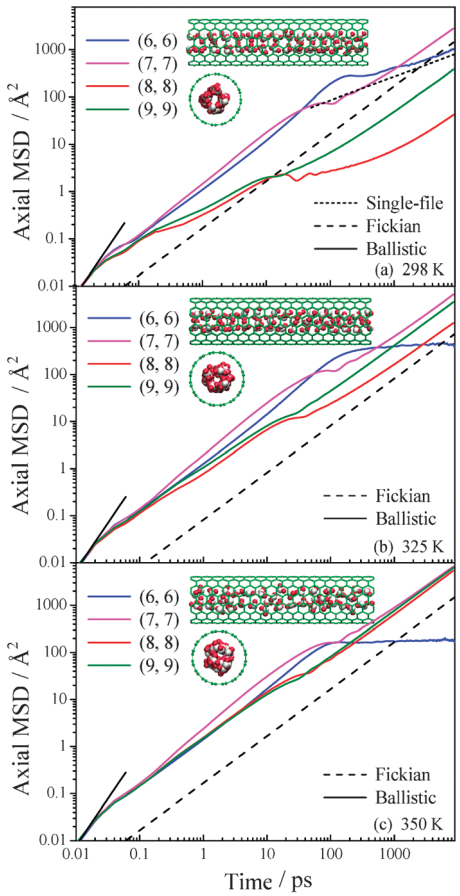

Fig. 3 The logarithmic plot of the axial MSD of the water molecules inside the small-diameter CNTs against the time at 298 K,[8] 325 K and 350 K. The insets show the structural configurations of water molecules inside the (8, 8) CNT at the three temperatures.

In the second stage (long-time diffusion), the diffusion mechanism inside the (6, 6) CNT becomes the single-file type at 298 K and then almost bends down to a constant at 325 K and 350 K. Inside the larger CNTs, the motions of water molecules approximately obey the Fickian diffusion mechanism in the long-time diffusion.

From Fig. 3, it can be found that the diffusion mechanism inside the (6, 6) CNT exhibits a peculiar change as the temperature increases. Though the water molecules inside the (6, 6) CNT arrange in chain-like structure, the single-file diffusion mechanism can only be observed in long-time diffusion at 298 K. As the temperature increases to 325 K and 350 K, the MSD eventually saturates to a constant. The single-file diffusion arises from the existence of the multi-chain structure, among which the vacancies provide enough spaces for the motions of water molecules.[8] When the temperature rises to 325 K and 350 K, the amount of the vacancies sharply reduces due to the uniform distribution of water molecules resulting from the high frequency and amplitude of molecular thermal motions. Thus, the water molecules are almost evenly spaced one by one and only move rightward and leftward within a certain distance, which will lead to a saturated MSD in long time limit.

The appearance of the two-stage diffusion mechanism can be ascribed to two factors, *i.e.*, the small confinement and the

periodic surface. On the one hand, the small confinement of size comparable to the molecular diameter suppresses the radial motions of the water molecules, which restricts the exchanges and results in frequent collisions in the axial direction in short time. The crossover in the MSD–t curve actually reflects the average time of the collisions between the adjacent molecules.[22,23,26] For the single-file transport, this shifting time can be calculated by $\tau_d = (D\rho^2)^{-1}$, in which D is the diffusion coefficient and $\rho = N/L$ (N, $L \to \infty$) is the constant number density along the axial direction.[22,23,26,33] It is assumed that the above formula is still valid for the water confined in the small-diameter CNTs. Using D = 0.05–0.4 Å^2 ps^{-1} (see the next section) and an approximate number density $\rho \approx 0.37$ Å^{-1} (the average distance between the water molecules confined in small-diameter CNTs is about 2.7 Å[38,39]), we can estimate that $\tau_d \approx$ 18–146 ps, which is almost consistent with the present simulation results in Fig. 3. On the other hand, the periodic interactions from the topological structure of CNT surfaces should also be responsible for the two-stage diffusion mechanism. Under the periodic interaction effect, the water molecules cannot achieve the continuous and uniform motions. This leads to the difference between the short-time motions and the long-time motions (inset of Fig. 4) and therefore results in different diffusion mechanisms in the two stages. The role of the periodic surface can be substantiated by the temperature dependence of the crossover in the MSD–t curves. From Fig. 4, it can be seen that as the temperature increases, the absolute value of the potential energy occupied by carbon atoms decreases. Correspondingly, the crossovers in the MSD–t curves become obscure with the decrease in the interactions between the CNT surfaces and the water molecules. Moreover, the previous MD simulations of LJ fluids pointed out that the unstructured tube cannot but the tube structured by a periodic potential can result in the single-file diffusion in long-time diffusion,[32] which implies that the periodic surface can influence the diffusion behavior. The theoretical calculations for the diffusion of single-file particles inside a nanochannel with a sinusoidal substrate surface also indicated that the crossover in the MSD curve gradually disappears as the effective substrate strength decreases.[26] This qualitative relation between the crossover and the surface–fluid interaction is consistent with the present discussion, which can be utilized to understand the dependence of the shift extent on the temperature in Fig. 3.

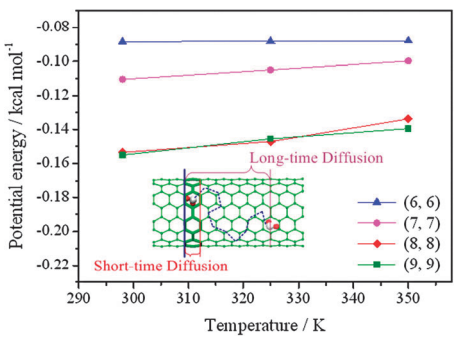

Fig. 4 The potential energy of the carbon atom of the small-diameter CNTs at the three temperatures. The inset illustrates the effect of the periodic CNT surface on the short-time diffusion.

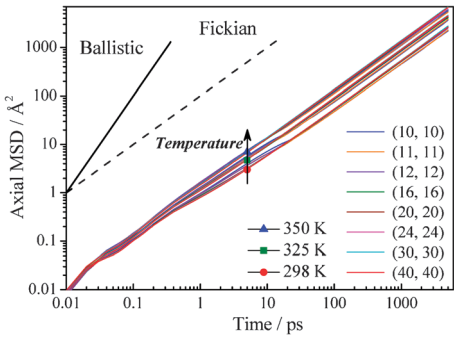

Fig. 5 The logarithmic plot of the axial MSD of the water molecules inside the large-diameter CNTs against the time at 298 K,[8] 325 K and 350 K.

Consequently, the two-stage diffusion mechanism inside the small-diameter CNTs is induced by the cooperation of the small confinement and the periodic surface.

The axial MSD of the water molecules inside the large-diameter (>13.56 Å) CNTs at the three temperatures is illustrated in Fig. 5, which is still presented in logarithmic scale for clearly distinguishing the diffusion mechanism. The representative lines of the ballistic and the Fickian diffusion mechanisms are also plotted in the figure for comparison. It can be seen that the water molecules initially follow the ballistic mechanism and then become of the Fickian-type diffusion. Some fluctuations can be found in the short-time MSD curves, which are quite slight compared with those inside the small-diameter CNTs and do not obviously affect the linear MSD–t relations. Moreover, it is notable that the increase in the temperature does not induce an evident change in the diffusion mechanism of water molecules inside the large CNTs. The present diffusion mechanism is similar to the intrinsic diffusion mechanism of bulk water (Fickian diffusion). It is suggested that the radial confinement larger than 13.56 Å almost cannot suppress the relative motions of water molecules so that they can easily pass each other along the axial direction. As for the effect of periodic surface, it is rather weak because the surface-to-volume ratio becomes small for these large CNTs. The weakening of these two effects leads to the appearance of the intrinsic diffusion mechanism inside the large-diameter CNTs.

4. Diffusion coefficient

The mobility of the water molecules inside CNTs can be examined by the diffusion coefficient, which is calculated by[35,40]

$$D = \lim_{t\to\infty} \frac{1}{2dt} \langle |\vec{r}(t) - \vec{r}(0)|^2 \rangle \qquad (2)$$

where d is the degree of dimensions. Fig. 6 shows the variations of the axial diffusion coefficient of the water molecules confined in CNTs at the three temperatures with respect to the diameter. The dashed lines denote the diffusion coefficients of bulk water, 2.49 × 10^{-9} m^2 s^{-1} at 298 K, 4.12 × 10^{-9} m^2 s^{-1} at 325 K and 6.05 × 10^{-9} m^2 s^{-1} at 350 K. These results are in agreement with the relevant results in the previous studies.[35] In Fig. 6, the diffusion coefficients inside the (6, 6) CNT at the

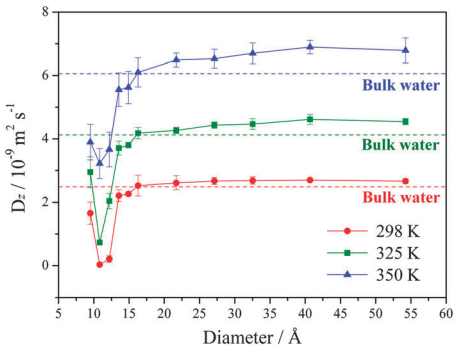

Fig. 6 The axial diffusion coefficient of the water molecules inside the CNTs at 298 K,[8] 325 K and 350 K. The dashed lines represent the corresponding diffusion coefficients of bulk water.

three temperatures are not presented. This is because that the diffusion coefficients at 325 K and 350 K cannot be calculated through eqn (2) owing to the non-linear MSD–t relation. While at 298 K, only the single-file mobility of the water molecules inside the (6, 6) CNT can be obtained, *i.e.*, 5.4×10^{-14} m^2 s$^{-0.5}$.[8] As for the (7, 7), (8, 8) and (9, 9) CNTs, the diffusion coefficient in the long-time diffusion is calculated through the linear MSD–t relation in the last 6.5 ns. From the figure, it can be found that for the same CNTs, the diffusion coefficient of the confined water increases as the temperature increases. For the same temperatures, except for the (8, 8) and (9, 9) CNTs, the diffusion coefficient increases with increasing diameter up to about 40 Å, and then gradually approaches the corresponding diffusion coefficient of bulk water. It should be noted that compared to the diffusion coefficient of bulk water, the CNTs of diameter larger than 16 Å could result in a slight enhancement in the diffusion coefficient of water. As for the diffusion coefficients inside the (8, 8) and (9, 9) CNTs, a sharp reduction can be observed, which is induced by the strong coupling strength among the water molecules due to the structural configurations (see the insets in Fig. 3).

It can be seen from the calculated results that the diffusion coefficient of the confined water exhibits some anomalous trends, including the nonmonotonic variation and the unexpected enhancement. The appearance of these phenomena should be ascribed to the competition of the smooth surface and the small confinement of CNTs. To further understand the double-edged effect of CNTs, taking the (20, 20) CNT as a standard, two groups of numerical examples are carried out to explore the roles of the surface effect and the confinement effect in the diffusion coefficient, respectively.

Firstly, for the surface effect, based on the (20, 20) CNT, three LJ potential depths $\varepsilon'_{CO} = 0.10648\,(0.9\,\varepsilon_{CO})$, 0.11831 (1.0 ε_{CO}) and 0.13014 (1.1 ε_{CO}) kcal mol^{-1} are considered to construct the nanotubes with different surface adsorptive capacities. Such variations in the LJ interactions can be achieved through coating the CNT surfaces or adopting the other nanotubes (such as the boron nitride nanotubes).[41–45] To examine the adsorptive capacities of the CNT surfaces with the different LJ potential depths, we firstly perform a direct calculation of the LJ potential of a water molecule sliding over a graphene, as shown in Fig. 7. The distance between the water molecule and the graphene (d in Fig. 7) is 2.94 Å, which

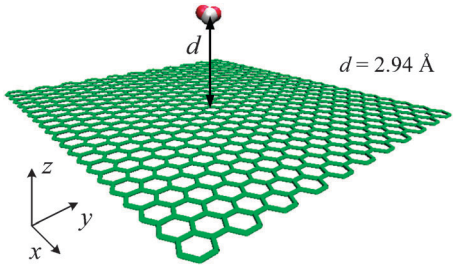

Fig. 7 The computational model of the adsorptive capacity of hexagonal atomic rings.

equals to the position of the first peak in the radial distribution function of water inside the (20, 20) CNT. The three insets in Fig. 8 illustrate the LJ potential of the water molecule over the graphenes with the three LJ potential depths, respectively. It can be seen that the adsorptive capacity of the hexagonal carbon rings gets stronger with an increase in the potential depth, implying that the CNT with a smaller potential depth will provide a smoother surface. Fig. 8 gives the variations of the relative diffusion coefficient with respect to the temperatures. Here, the relative diffusion coefficient is the ratio of the calculated diffusion coefficient to the diffusion coefficient of bulk water at the corresponding temperatures. From Fig. 8, we can find that the relative diffusion coefficient is almost linearly dependent on the temperature for the same CNT surface. The slope of curves should be relevant to the smooth extents of the CNT surfaces. As for the same temperature, the diffusion coefficient decreases with increasing LJ potential depth, and the drops in the diffusion coefficient become more remarkable at the higher temperature. These results demonstrate that the smooth surface can provide a fast path for the motions of water molecules at the boundary layers, which results in an enhancement in the diffusion coefficient of water. Moreover, it should be noted that such enhancement will become evident as the surface-to-volume ratio increases. Hence, the surface-driven enhancement in the diffusion coefficient of the confined water can be assumed through a simple qualitative relation as follows

$$\frac{D_z}{D_T} \propto T\frac{l}{S} \tag{3}$$

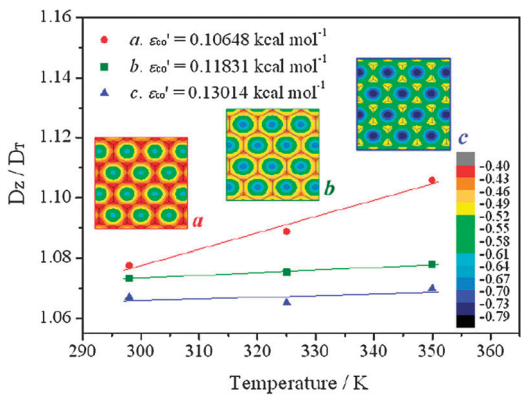

Fig. 8 The relative diffusion coefficient of the water molecules confined in the nanotubes with the surfaces of different adsorptive capacities against the temperature. The insets show the potential energy of the water molecule sliding over the hexagonal atomic rings (kcal mol^{-1}).

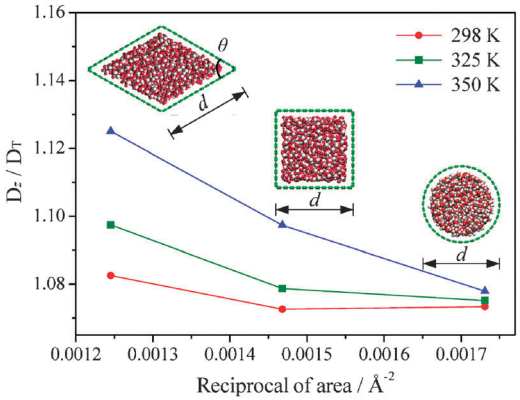

Fig. 9 The relative diffusion coefficient of the confined water inside the three kinds of CNTs *versus* the reciprocal of area. The insets show the cross-sections of the three kinds of CNTs.

in which D_T is the diffusion coefficient of bulk water at temperature T, and l and S are the perimeter and the cross-sectional area of CNTs, respectively.

Secondly, the confinement effect is studied through three kinds of CNTs with the same ratio of surface to volume but different cross-sectional shapes. The objective of adopting the same ratio is to eliminate the surface effect. The three kinds of CNTs are of the diamond, the rectangular and the circular cross-sections, respectively, as shown in insets of Fig. 9. The nanotubes with special cross-sectional shapes have been reported in some previous works.[46,47] In this paper, the CNT with the circular cross-section corresponds to the normal (20, 20) CNT. The other two special CNTs are, respectively, called the diamond CNT and the square CNT, which are constructed through unfolding a graphene of specified size. The present computation is just to check the confinement effect though the established models of the two special CNTs may be unrealistic. The lengths of the three CNTs are 103.3 Å. The water density in the two special kinds of CNTs is calculated by a preparative MD simulation, in which two water reservoirs are introduced to provide a natural hydrostatic pressure. The detailed sizes of the three CNTs and the densities of the enclosed water are shown in Table 2. According to Table 2, it can be seen that the cross-sectional areas of the diamond, the square and the normal CNTs decrease in turn, which implies a reduction in the confinement effect. The relative diffusion coefficients of the water molecules confined in various CNTs at the three temperatures are shown in Fig. 9. The computational results reveal that the relative diffusion coefficient of the confined water decreases with decreasing cross-sectional area (from the diamond to the circle CNTs) at the same temperatures.

Table 2 The detailed sizes of the three CNTs and the densities of the enclosed water

Cross-section		Diamond	Square	Circle
Size/Å		d = 30.45, θ = 60°	d = 26.10	d = 27.12
Perimeter/Å		121.80	104.40	85.20
Area/Å^2		802.98	681.21	577.66
Ratio/Å^{-1}		0.152	0.153	0.147
Water density/ g cm^{-3}	298 K	0.71	0.71	0.72
	325 K	0.70	0.69	0.71
	350 K	0.68	0.67	0.70

The present computation indicates that the small confinement will restrict the free motions of the water molecules, which reduces the diffusion coefficient. Provided that the confinement can produce a linear effect in the diffusion coefficient, we can gain a qualitative relation describing the confinement-driven reduction in the diffusion coefficient

$$\frac{D_z}{D_T} \propto \frac{1}{S} \tag{4}$$

Here, it is considered that the confinement effect of nanotubes is only dominated by the geometrical property without temperature dependence. Moreover, the reciprocal in eqn (4) can ensure that the confinement effect gradually vanishes as the confinement size increases.

The above two numerical examples justify the enhanced role of the surface effect and the reduced role of the confinement effect in the diffusion coefficient. The competition of these two effects leads to the anomalous dependence of the diffusion coefficient on the diameter of CNTs. According to the qualitative relations, *i.e.*, eqn (3) and (4), the diffusion coefficient of the confined water can be fitted through

$$D_z = D_T\left(1 + \alpha T\frac{l}{S} - \beta\frac{1}{S}\right) \tag{5}$$

where the second term and third term correspond to the surface effect and the confinement effect on the diffusion coefficient, respectively. The sign of the third term is minus due to the reduced role of the confinement effect. The parameters α and β are two undetermined constants relating to the surface smoothness and the cross-sectional shape of nanochannel, respectively. Through fitting the results in Fig. 6, without consideration of the anomalous decreases in the (8, 8) and (9, 9) CNTs, we can determine that α = 0.00341 Å K^{-1} and β = 59 Å^2 for the CNTs. It is notable that the parameter β = 59 Å^2 is comparable with the cross-sectional area of the (6, 6) CNT (52 Å^2), which is the minimum CNT allowing the water molecules to enter. The magnitudes of the second and third terms in eqn (5) are displayed in Fig. 10. It can be seen that for the CNTs of diameter up to ~16 Å, the confinement effect dominates over the surface effect, which results in the decrease in the diffusion coefficient compared to that of bulk

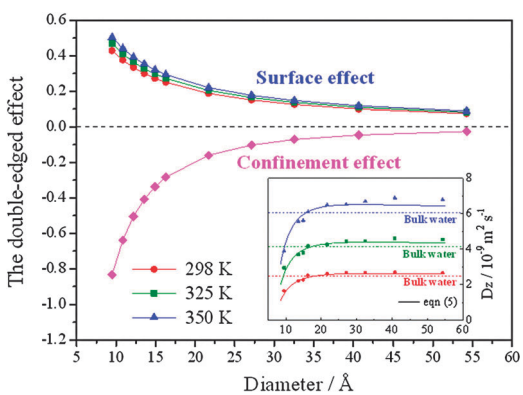

Fig. 10 The quantitative comparison of the surface effect and the confinement effect according to the second term and the third term in eqn (5). The inset illustrates the computational results of eqn (5).

water. Thereafter, the surface effect plays the dominant role, which leads to the slight increase in the diffusion coefficient. Eventually, both of the two effects vanish gradually with increasing diameter of CNTs. Moreover, it is notable that the surface effect slightly increases as the temperature increases, which can be used to interpret the growing increment of the diffusion coefficient of the confined water compared to that of bulk water with the temperature (see Fig. 6). The inset in Fig. 10 depicts the results calculated by eqn (5) (lines), whose correlation coefficient with the simulation results (symbols) is 0.97. The good agreement demonstrates the rationality of eqn (5).

5. Conclusion

In this paper, the temperature dependences of the diffusion mechanism and the diffusion coefficient of the water confined in CNTs are investigated by the MD simulations. The results revealed that the two features of CNTs, the nanoscale surface and the small confinement, can induce anomalous diffusion behaviors of the confined water. For the diffusion mechanism, the cooperation of the two effects results in the appearance of the two-stage diffusion mechanism inside the CNTs of diameter smaller than 12.2 Å. As for the diffusion coefficient, the competition of the two effects results in the nonmonotonic size dependence and the unexpected increase. Moreover, an estimation formula for the temperature-dependent diffusion coefficient is proposed. The present research provides an insight into understanding the flow behaviors inside nanochannels, which is instructive for the design and the fabrication of the nanofluidic devices.

Acknowledgements

The supports of the National Natural Science Foundation of China (11072051, 90715037, 10902021, 91015003, 10728205, 10721062), NSFC-JST (51021140004), the 111 Project (No. B08014), the National Key Basic Research Special Foundation of China (2010CB832704) and the Program for Changjiang Scholars and Innovative Research Team in University of China (PCSIRT) are gratefully acknowledged.

References

1 Z. G. Mao and S. B. Sinnott, A computational study of molecular diffusion and dynamic flow through carbon nanotubes, *J. Phys. Chem. B*, 2000, **104**, 4618.
2 A. Striolo, The mechanism of water diffusion in narrow carbon nanotubes, *Nano Lett.*, 2006, **6**, 633.
3 X. Chen, G. X. Cao, A. J. Han, V. K. Punyamurtula, L. Liu, P. J. Culligan, T. Kim and Y. Qiao, Nanoscale fluid transport: size and rate effects, *Nano Lett.*, 2008, **8**(9), 2988.
4 Y. C. Liu, J. D. Moore, T. J. Roussel and K. E. Gubbins, Dual diffusion mechanism of argon confined in single-walled carbon nanotube bundles, *Phys. Chem. Chem. Phys.*, 2010, **12**, 6632.
5 Y. X. Li, J. L. Xu and D. Q. Li, Molecular dynamics simulation of nanoscale liquid flows, *Microfluid. Nanofluid.*, 2010, **9**, 1011.
6 H. J. Park and N. R. Aluru, Ordering-induced fast diffusion of nanoscale water film on graphene, *J. Phys. Chem. C*, 2010, **114**, 2595.
7 H. W. Zhang, H. F. Ye, Y. G. Zheng and Z. Q. Zhang, Prediction of the viscosity of water confined in carbon nanotubes, *Microfluid. Nanofluid.*, 2011, **10**, 403.
8 H. F. Ye, H. W. Zhang, Y. G. Zheng and Z. Q. Zhang, Nanoconfinement induced anomalous water diffusion inside carbon nanotubes, *Microfluid. Nanofluid.*, 2011, **10**, 1359.
9 J. Martí and M. C. Gordillo, Temperature effects on the static and dynamic properties of liquid water inside nanotubes, *Phys. Rev. E: Stat., Nonlinear, Soft Matter Phys.*, 2001, **64**, 021504.
10 Y. C. Liu, Q. Wang and L. H. Lu, Density inhomogeneity and diffusion behavior of fluids in micropores by molecular-dynamics simulation, *J. Chem. Phys.*, 2004, **120**(22), 10728.
11 D. P. Cao and J. Z. Wu, Self-diffusion of methane in single-walled carbon nanotubes at sub- and supercritical conditions, *Langmuir*, 2004, **20**, 3759.
12 Y. C. Liu, Q. Wang and X. F. Li, A diffusion model for the fluids confined in micropores, *J. Chem. Phys.*, 2005, **122**, 044714.
13 H. F. Ye, H. W. Zhang, Z. Q. Zhang and Y. G. Zheng, Size and temperature effects on the viscosity of water inside carbon nanotubes, *Nanoscale Res. Lett.*, 2011, **6**, 87.
14 M. Majumder, N. Chopra, R. Andrews and B. J. Hinds, Enhanced flow in carbon nanotubes, *Nature*, 2005, **438**, 44.
15 J. K. Holt, H. G. Park, Y. M. Wang, M. Stadermann, A. B. Artyukhin, C. P. Grigoropoulos, A. Noy and O. Bakajin, Fast mass transport through sub-2-nanometer carbon nanotubes, *Science*, 2006, **312**, 1034.
16 A. Striolo, Water self-diffusion through narrow oxygenated carbon nanotubes, *Nanotechnology*, 2007, **18**(47), 475704.
17 M. P. Allen and D. J. Tildesley, *Computer simulation of liquids*, Clarendon Press, Oxford, 1987.
18 S. Jakobtorweihen, M. G. Verbeek, C. P. Lowe, F. J. Keil and B. Smit, Understanding the loading dependence of self-diffusion in carbon nanotubes, *Phys. Rev. Lett.*, 2005, **95**, 044501.
19 D. G. Levitt, Dynamics of a single-file pore: non-Fickian behavior, *Phys. Rev. A*, 1973, **8**, 3050.
20 Q. H. Wei, C. Bechinger and P. Leiderer, Single-file diffusion of colloids in one-dimensional channels, *Science*, 2000, **287**, 625.
21 K. K. Mon and J. K. Percus, Self-diffusion of fluids in narrow cylindrical pores, *J. Chem. Phys.*, 2002, **117**(5), 2289.
22 B. H. Lin, M. Meron, B. X. Cui and S. A. Rice, From random walk to single-file diffusion, *Phys. Rev. Lett.*, 2005, **94**, 216001.
23 F. Marchesoni and A. Taloni, Subdiffusion and long-time anticorrelations in a stochastic single file, *Phys. Rev. Lett.*, 2006, **97**, 106101.
24 L. Lizana and T. Ambjörnsson, Single-file diffusion in a box, *Phys. Rev. Lett.*, 2008, **100**, 200601.
25 A. Taloni and M. A. Lomholt, Langevin formulation for single-file diffusion, *Phys. Rev. E: Stat., Nonlinear, Soft Matter Phys.*, 2008, **78**, 051116.
26 P. S. Burada, P. Hänggi, F. Marchesoni, G. Schmid and P. Talkner, Diffusion in confined geometries, *ChemPhysChem*, 2009, **10**, 45.
27 A. Das, S. Jayanthi, H. S. M. V. Deepak, K. V. Ramanathan, A. Kumar, C. Dasgupta and A. K. Sood, Single-file diffusion of confined water inside SWNTs: an NMR study, *ACS Nano*, 2010, **4**, 1687.
28 B. Mukherjee, P. K. Maiti, C. Dasgupta and A. K. Sood, Single-file diffusion of water inside narrow carbon nanorings, *ACS Nano*, 2010, **4**, 985.
29 B. Mukherjee, P. K. Maiti, C. Dasgupta and A. K. Sood, Strong correlations and Fickian water diffusion in narrow carbon nanotubes, *J. Chem. Phys.*, 2007, **126**, 124704.
30 T. Nanok, N. Artrith, P. Pantu, P. A. Bopp and J. Limtrakul, Structure and dynamics of water confined in single-wall nanotubes, *J. Phys. Chem. A*, 2009, **113**, 2103.
31 K. E. Gubbins, Y. C. Liu, J. D. Moore and J. C. Palmer, The role of molecular modeling in confined systems: impact and prospects, *Phys. Chem. Chem. Phys.*, 2011, **13**, 58–85.
32 K. Hahn and J. Kärger, Molecular dynamics simulation of single-file systems, *J. Phys. Chem.*, 1996, **100**, 316–326.
33 K. Hahn and J. Kärger, Deviations from the normal time regime of single-file diffusion, *J. Phys. Chem. B*, 1998, **102**, 5766–5771.
34 R. J. Mashl, S. Joseph, N. R. Aluru and E. Jakobsson, Anomalously immobilized water: a new water phase induced by confinement in nanotubes, *Nano Lett.*, 2003, **3**(5), 589.
35 W. H. Hans, C. S. William, W. P. Jed, D. M. Jeffry, J. D. Thomas, L. H. Greg and H. G. Teresa, Development of an improved

four-site water model for biomolecular simulations: TIP4P-EW, *J. Chem. Phys.*, 2004, **120**, 9665.
36 S. Plimpton, Fast parallel algorithms for short-range molecular dynamics, *J. Comput. Phys.*, 1995, **117**, 1 (http://lammps.sandia.gov).
37 J. P. Bouchaud, A. Georges, J. Koplik, A. Provata and S. Redner, Superdiffusion in random velocity fields, *Phys. Rev. Lett.*, 1990, **64**, 2503.
38 G. Hummer, J. C. Rasaiah and J. P. Noworyta, Water conduction through the hydrophobic channel of a carbon nanotube, *Nature*, 2001, **414**(8), 188.
39 A. Berezhkovskii and G. Hummer, Single-file transport of water molecules through a carbon nanotube, *Phys. Rev. Lett.*, 2002, **89**(6), 064503.
40 D. C. Rapaport, *The art of molecular dynamics simulation*, Cambridge University Press, New York, 2004.
41 Y. Zhang, N. W. Franklin, R. J. Chen and H. J. Dai, Metal coating on suspended carbon nanotubes and its implication to metal-tube interaction, *Chem. Phys. Lett.*, 2000, **331**, 35.
42 R. Nap and I. Szleifer, Control of carbon nanotube-surface interactions: the role of grafted polymers, *Langmuir*, 2005, **21**, 12072.
43 P. A. Gauden, A. P. Terzyk, R. Pieńkowski, S. Furmaniak, R. P. Wesołowski and P. Kowalczyk, Molecular dynamics of zigzag single walled carbon nanotube immersion in water, *Phys. Chem. Chem. Phys.*, 2011, **13**, 5621.
44 N. G. Chopra, R. J. Luyken, K. Cherrey, V. H. Crespi, M. L. Cohen, S. G. Louie and A. Zettl, Boron nitride nanotubes, *Science*, 1995, **269**, 966.
45 J. Köfinger, G. Hummer and C. Dellago, Single-file water in nanopores, *Phys. Chem. Chem. Phys.*, 2011, **13**, 15403–15417.
46 R. Q. Zhang, H. L. Lee, W. K. Li and B. K. Teo, Investigation of possible structures of silicon nanotubes *via* density-functional tight-binding molecular dynamics simulations and *ab initio* calculations, *J. Phys. Chem. B*, 2005, **109**, 8605.
47 F. Xu, J. E. Wharton and C. R. Martin, Template synthesis of carbon nanotubes with diamond-shaped cross sections, *Small*, 2007, **10**, 1718.